JOURNAL OF CATALYSIS 83, 50–60 (1983)

Effects of Impregnation pH on the Surface Structure and Hydrodesulfurization Activity of Mo/Al_2O_3 Catalysts

MARWAN HOUALLA,*,† CHARLES L. KIBBY,* LEONIDAS PETRAKIS,*,† AND DAVID M. HERCULES†

*Department of Chemistry, University of Pittsburgh, Pittsburgh, Pennsylvania 15260 and †Gulf Research and Development Company, P.O. Drawer 2038, Pittsburgh, Pennsylvania 15230

Received November 2, 1982; revised April 26, 1983

A series of Mo/Al_2O_3 catalysts was prepared by incipient wetness impregnation at various pH's (4.0, 5.4, 7.1, and 11.0) using a fixed amount of Mo (8% Mo). The effect of pH on the state and dispersion of Mo species in the dried, calcined, and reduced catalysts was investigated by the combined use of two surface sensitive techniques: X-ray photoelectron spectroscopy (XPS, ESCA) and ion scattering spectroscopy (ISS). The surface properties were correlated to thiophene hydrodesulfurization activities for the various catalysts. A tentative interpretation of the influence of pH of the Mo impregnating solution on the surface structure of Mo/Al_2O_3 catalysts at various stages of their preparation is proposed.

INTRODUCTION

Hydrodesulfurization (HDS) catalysts have been the subject of extensive investigation (*1–3*) aimed at achieving a better understanding of the nature of the active phase. A typical HDS catalyst consists, in its precursor form, of Mo (or W) deposited by incipient wetness impregnation on a high surface area transition alumina (γ,η). A survey of recent literature concerning HDS catalysts shows that great effort has been expended on characterization of the calcined oxidic states, while less attention has been given to assessing the effect of Mo impregnation conditions on the properties of the final catalyst. An early, systematic study of some preparation conditions of model HDS catalysts provided strong indication that there may be significant variations in the structure and behavior of the final catalyst depending on the exact preparation procedure used (*4*). For example, the nature of Mo species, their dispersion, and interaction with the alumina carrier may well be determined by the pH of the Mo impregnating solution (*5*).

The purpose of the present study was to investigate, by combined use of X-ray photoelectron spectroscopy (ESCA) and ion scattering spectroscopy (ISS), the influence of the Mo impregnating solution pH on the state and dispersion of the Mo phase in the various sequences of catalyst production (drying, calcination, and reduction). The catalyst surface structures, thus determined, were correlated with their HDS activities.

EXPERIMENTAL

Materials

A series of Mo/Al_2O_3 samples was prepared by pore volume impregnation of a Ketjen CK.300 γ-Al_2O_3 (surface area 200 m^2/g, pore volume 0.6 cm^3/g, 20–40 mesh) with solutions of ammonium heptamolybdate at various pH's (4.0, 5.4, 7.1, and 11.0) using a fixed amount of molybdenum (8.1 wt% Mo). The solution pH's were adjusted with HNO_3 or NH_4OH. The samples were dried at 120°C for 16 h and calcined at 500°C for 16 h. The dried, calcined, and reduced catalysts series are designated, respectively, MoAl(D*x*), MoAl(C*x*) and MoAl (R*x*), where *x* is the pH of the heptamolybdate solution used for impregnation. As indicated by Table 1, the BET surface area of

0021-9517/83 $3.00

TABLE 1

Surface Areas of Calcined Molybdena–Alumina Catalysts

pH of Mo impregnation	Surface area (m^2/g)
4.0	192
5.4	186
7.1	187
11.0	198
unimpregnated	200

the alumina carrier was little affected by Mo deposition or by the pH of the Mo impregnating solution.

Surface Characterization

ESCA operating procedure. ESCA spectra were acquired with an AEI ES200 spectrometer interfaced to a DS200 data system. The spectrometer is equipped with an aluminum anode (Al$K\alpha$ = 1486.6 eV), operated at 12 kV and 22 mA. The residual pressure inside the spectrometer was 2×10^{-8} Torr. The samples were either finely ground and dusted on double-sided adhesive tape or, when heat treatment was needed, pressed into pellets at 7000 kg/cm^2 and mounted on a sealable probe. Binding energies were referenced to Al 2*p* line at 74.5 eV.

Basis for quantitative intensity measurements. ESCA signal intensities (photoelectrons counted per unit time) are represented by the areas under the corresponding peaks. The background signal produced by inelastically scattered electrons was assumed to vary linearly with energy. The ESCA relative intensity measurements reported here concern the ratios of the intensities of two peaks, I_m and I_s, associated with the supported phase $\langle\langle MoO_3 \rangle\rangle$ and the alumina carrier, respectively. Several models have been proposed to correlate measured ESCA intensity ratios with dispersion of the supported phase (*6–9*). They take into account the support surface area and the shapes of the carrier and active phase particles. For monolayer coverage, assuming sheetlike structures for the carrier particles, it was shown that the predicted intensity ratio may be expressed by Eq. (1):

$$\frac{I_m^\circ}{I_s^\circ} = \frac{n_m}{n_s} \cdot \frac{D_m}{D_s} \cdot \frac{\sigma_m}{\sigma_s} \cdot \frac{1}{\rho_s S_s \lambda_s} \cdot \frac{(1 + \exp\{-2/\sigma_s \lambda_m S_s\})}{(1 - \exp\{-2/\sigma_s \lambda_m S_s\})} \quad (1)$$

where n_m/n_s is the atomic ratio of the characteristic elements representative of the supported phase (m = Mo) and carrier (s = Al). D_m and D_s are the detector efficiencies for the corresponding photoelectrons (Mo 3*d*, Al 2*p*). In the AEI instrument, the efficiencies are proportional to the electron kinetic energies. The photoelectron cross sections, σ_m for the Mo 3*d* ($\frac{3}{2}$, $\frac{5}{2}$) level and σ_s for the Al 2*p* level, were taken from Scofield (*10*). Photoelectron escape depths, λ_m for Mo 3*d* and λ_s for Al 2*p* electrons, were estimated to be 1.6 and 1.8 nm, respectively (*11*). The density of the carrier is ρ = 3.8 g/cm^3; S = 200 m^2/g is the specific surface area of the support.

When the active phase is present as discrete particles (for instance as cubic crystallites) on the carrier, the ESCA intensity ratio I_m/I_s may be expressed as a function of the particle size and the predicted intensity ratio for a monolayer (given by Eq. (1)). Defining the average cubic crystallite edge length as c, the intensity ratio is given by Eq. (2):

$$\frac{I_m}{I_s} = \frac{I_m^\circ}{I_s^\circ} \cdot \frac{(1 - \exp\{-c/\lambda_m\})}{c/\lambda_m}. \quad (2)$$

Equation (2) shows that I_m/I_s remains constant if the particle size of the deposited species does not vary, but it increases in the case of an enhanced dispersion of the active phase.

Finally, when the supported phase and the carrier form a homogeneous compound or a solid solution, Eq. (3) is followed:

$$\frac{I_m}{I_s} = \frac{n_m}{n_s} \cdot \frac{D_m}{D_s} \cdot \frac{\sigma_m}{\sigma_s} \cdot \frac{\lambda_m}{\lambda_s}. \quad (3)$$

It must be noted that quantitative analysis of ESCA intensity measurements, relative to a series of samples on a porous support, is valid only when no variation of the partitioning of the deposited phase takes place (e.g., amounts of the phase deposited inside the pores relative to amounts at the external parts of the carrier particles (*12*).

ISS. ISS spectra were recorded using a 3M model 525 ion scattering spectrometer; $^4He^+$ ions were used as a probe. The energy of the incident beam was 2 KeV. The current density was 1×10^{-7} A/cm^2. The energy of backscattered ions was measured with a cylindrical mirror analyzer. The residual pressure was 5×10^{-9} Torr. After backfilling the chamber with the scattering gas, the pressure was 1×10^{-5} Torr. The samples were pressed into pellets at 7000 kg/cm^2 and mounted on the probe for ISS analysis.

Reduction and HDS Activity Studies

Reduction measurements were carried out at 500°C for 30 min in a 40-cm^3/min flow of H_2. HDS activities of Mo/Al_2O_3 samples were determined for thiophene hydrodesulfurization at 300°C and 750 Torr in a fixed bed microreactor, with thiophene injected into a hydrogen carrier gas at a flow rate of 0.72 ml (g-catalyst) (h). Activation of the oxidic catalyst was achieved by prereduction with H_2 at 300°C and sulfidation with the reactant mixture (ca. 0.5% thiophene in H_2). Preliminary experiments showed that the variation of thiophene hydrogenolysis rate with thiophene pressure was approximately half-order at the pressures (ca. 15 Torr) and conversions (10–20%) used.

RESULTS

Dried Molybdena–Aluminas, MoAl(Dx) Series

ISS. Figure 1 shows typical ISS spectra for various MoAl(D*x*) samples. They all exhibit three peaks at $E/E_0 = 0.41$, 0.58, and 0.87, respectively, ascribed to O, Al, and Mo. The presence in all specimens of a significant aluminum peak at the onset of sputtering illustrates the submonolayer coverage of the MoAl(D*x*) samples.

Variation of the $I_{(Mo)}/I_{(Al)}$ ratio for the dried catalysts, as a function of the pH of the Mo impregnating solution, is shown in

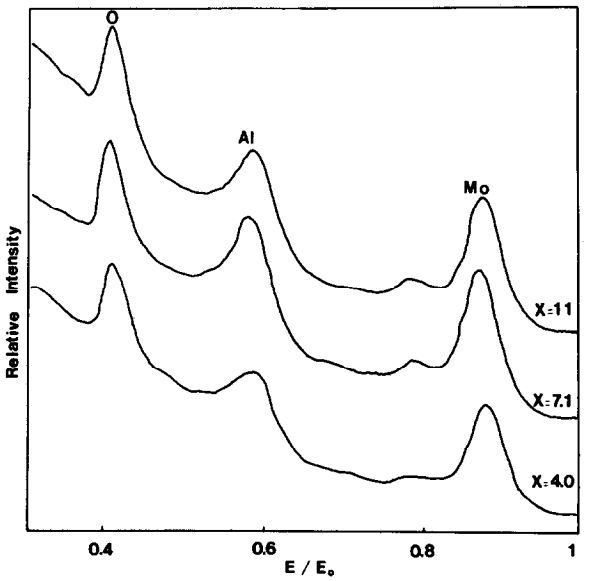

FIG. 1. Typical ISS spectra of dried Mo/Al_2O_3 catalysts: X is the pH of the Mo impregnating solution.

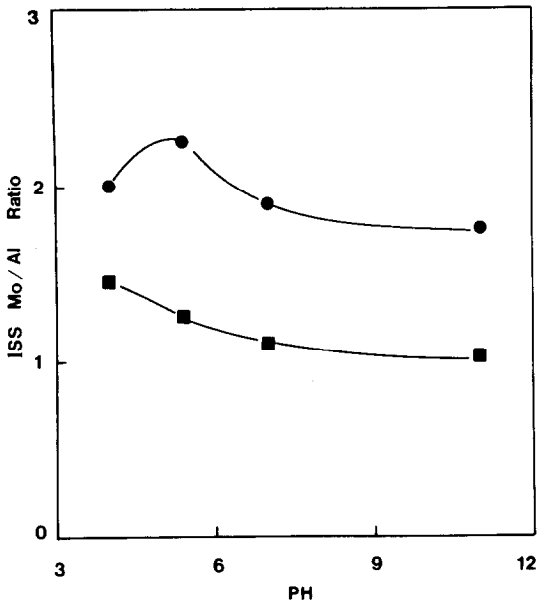

FIG. 2. Variation of the ISS intensity ratio I_{Mo}/I_{Al} as a function of pH of the Mo impregnating solution: ■ dried Mo/Al_2O_3 (D); ● calcined Mo/Al_2O_3 (C).

Fig. 2. The experimental points are the values of the intensity ratio measured after 20 min of sputtering. There is a steady and significant decrease of the $I_{(Mo)}/I_{(Al)}$ intensity ratio as the pH of Mo impregnation is increased.

ESCA. The binding energy values (232.8 eV) for the Mo $3d_{5/2}$ level in MoAl(Dx) samples is little affected by the pH of impregnation. Variations in the ESCA intensity ratio $I_{(Mo\ 3d)}/I_{(Al\ 2p)}$ as a function of pH are shown in Fig. 3 for the dried catalyst. There is first a small increase in the $I_{(Mo)}/I_{(Al)}$ ratio, then a steady decline, as the pH of impregnation is increased.

Calcined Molybdena–Aluminas, MoAl (Cx) Series

ISS. ISS spectra for various MoAl(Cx) samples were similar to those reported for the dried series (Fig. 1). Figure 2 shows the variation of the $I_{(Mo)}/I_{(Al)}$ intensity ratio of calcined Mo/Al_2O_3 samples as a function of the pH of the impregnating solution. Comparison of these ratios with those obtained for the dried samples (Fig. 2-(D)) shows that a noticeable increase of $I_{(Mo)}/I_{(Al)}$ occurs as a consequence of calcination. On the other hand, variation of the $I_{(Mo)}/I_{(Al)}$ ratio as a function of impregnation pH shows that with increasing pH, there is a slight

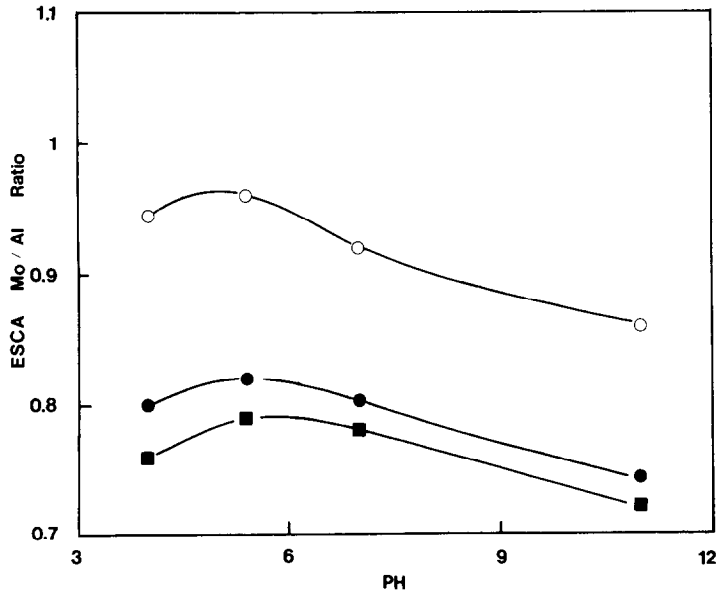

FIG. 3. Variation of ESCA intensity ratio $I_{Mo\ 3d}/I_{Al\ 2p}$ as a function of pH of the Mo impregnating solution: ● dried (D); ○ calcined (C); ■ reduced (R).

increase of the intensity ratio for the calcined catalysts, and then a steady decrease as is observed for the ESCA intensity ratio (Fig. 3).

ESCA. ESCA spectra and binding energies of Mo 3*d* levels for the MoAl(Cx) series were nearly identical to those obtained for the dried catalysts. A typical spectrum is shown in Fig. 4-(C). Figure 3 shows the variation with pH of the ESCA intensity ratio $I_{(Mo\ 3d)}/I_{(Al\ 2p)}$ for the dried and calcined specimens. In agreement with the ISS data, higher ESCA intensity ratios are obtained for the calcined samples, compared with the corresponding dried specimens. Furthermore, variation of the $I_{(Mo)}/I_{(Al)}$ ESCA ratio for the MoAl(C*x*) series follows the same trend measured by ISS (Fig. 2-(C)), namely, a slight enhancement of $I_{(Mo)}/I_{(Al)}$ when the pH is increased from 4.0 to 5.4, and a progressive decline as the pH is further increased.

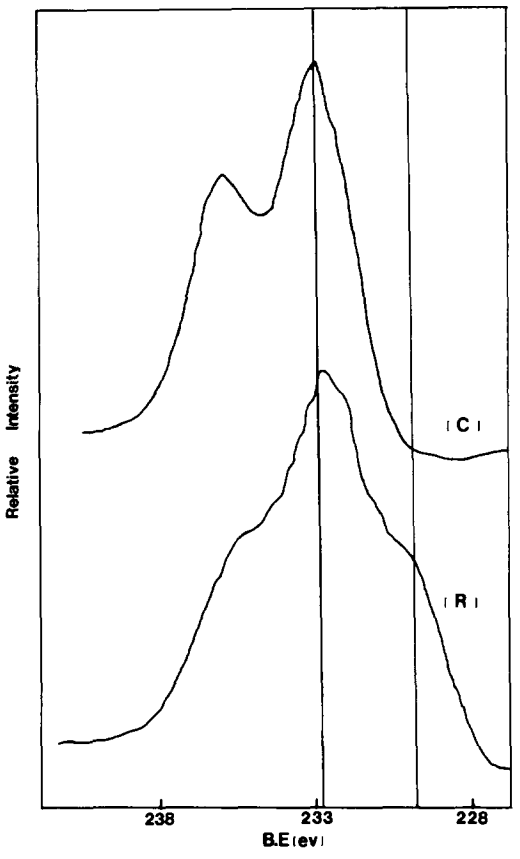

FIG. 4. Mo 3*d* ESCA spectra of (C) oxidic and (R) reduced calcined Mo/A_2O_3 catalysts; pH of Mo impregnating solution = 4; the vertical lines denote, respectively, the approximate B. E. (binding energy) positions for Mo^{6+} (232.8 eV) and Mo^{4+} (229.7 eV).

Reduced Molybdena–Aluminas, MoAl(Rx) Series

The Mo 3*d* spectrum of a reduced sample, MoAl(R4), is compared in Fig. 4 to that of the corresponding calcined specimen MoAl(C4). The most prominent modification resulting from the reduction treatment is the appearance of a peak at 229.7 eV binding energy, ascribed to Mo^{4+} (*13*). Furthermore, the shift to lower binding energies (ca. 232.5 eV) of the peak attributed to Mo^{6+} initially at 232.8 eV, may be taken as an indication of the formation of Mo^{5+}, with a binding energy about 232.2 eV (*13*). ESCA spectra of Mo 3*d* levels for various MoAl(R*x*) samples are shown in Fig. 5. It is clear that variation of the pH of the Mo impregnating solution had little impact on the distribution of the Mo oxidation states on reductions. Based on an earlier study of the reduction of Mo/Al_2O_3 catalysts (*13*), one may assume that under the reduction conditions adopted here, the Mo 3*d* envelope is the result of contributions from Mo^{5+} and Mo^{4+} peaks. Their relative percentages, thus determined (60 and 40%, respectively) are comparable to those previously reported (*13*).

Figure 3 shows the variation with pH of the ESCA intensity ratio $I_{(Mo\ 3d)}/I_{(Al\ 2p)}$ for reduced samples. It is apparent that the pattern exhibited by the dried and calcined samples is maintained after reduction. However, it is also evident that the reduction treatment brings about a decrease in the $I_{(Mo\ 3d)}/I_{(Al\ 2p)}$ ratios, relative to calcined specimens.

HDS Activity

The oxide forms, mildly reduced at 300°C, were initially very poor catalysts. They became active as they were sulfided during the thiophene conversion, reaching

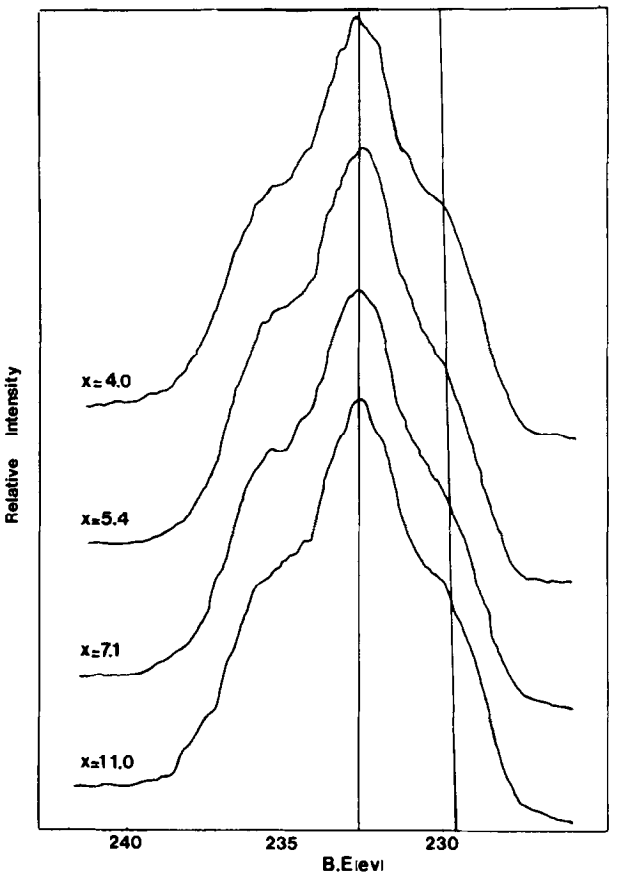

FIG. 5. ESCA spectra of the Mo 3*d* level in reduced Mo/Al_2O_3 catalysts: X is the pH of the Mo impregnating solution.

a maximum activity after about 2 h of operation, as shown in Fig. 6. The activity slowly declined overnight and remained fairly constant after 20 h.

Variations of the relative values of steady state thiophene HDS activity for the MoAl(C*x*) catalysts, expressed as half-order rate constants vs pH, are shown in Fig. 7. It is evident that better HDS activities are obtained for catalysts prepared at low pH. Those catalysts also reached a higher level of activity more rapidly (Fig. 6). The activity pattern is comparable to the pattern observed for the corresponding ESCA and ISS intensity ratios also shown in Fig. 7.

DISCUSSION

In the following discussion, we will first evaluate the overall influence of calcination and reduction treatments on the dispersion and surface structure of the Mo/Al_2O_3 catalysts. We will then examine the effects of the pH of the Mo impregnating solution on the surface composition of Mo/Al_2O_3 samples and how this relates to their HDS activities. Finally, a tentative interpretation of the pH effect will be proposed.

As stated in the experimental section, the variations of ESCA (and ISS) intensity ratios (I_{Mo}/I_{Al}) will reflect any modifications of the dispersion of the supported phase, only when no variation of the "partitioning" of the deposited phase takes place. Mo/Al_2O_3 catalysts prepared by dry impregnation of Al_2O_3 extrudate have indeed been shown (*14, 15*) to exhibit a significant enrichment in Mo at the outer part of the particle compared to the bulk. Thus, one must ascertain

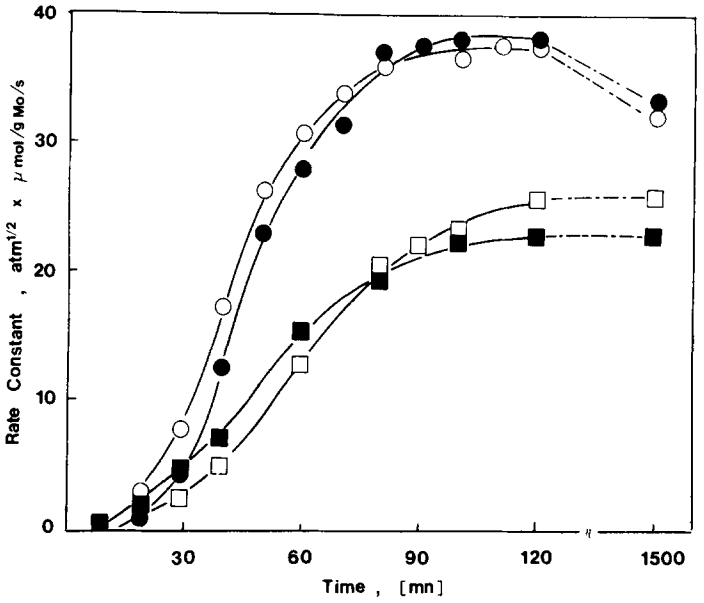

FIG. 6. Activation of molybdena–aluminas with time during thiophene hydrogenolysis: ○ pH = 4; ● pH = 5.4; □ pH = 7.1; ■ pH = 11.

that such variations of the intensity ratio (I_{Mo}/I_{Al}) observed as a function of pH are not simply the results of alterations of the repartition of the Mo phase. This has been achieved by comparing the ESCA intensity ratio of I_{Mo}/I_{Al} of ground and unground samples (50–70 mesh). The results show that both series exhibit similar intensity ratios

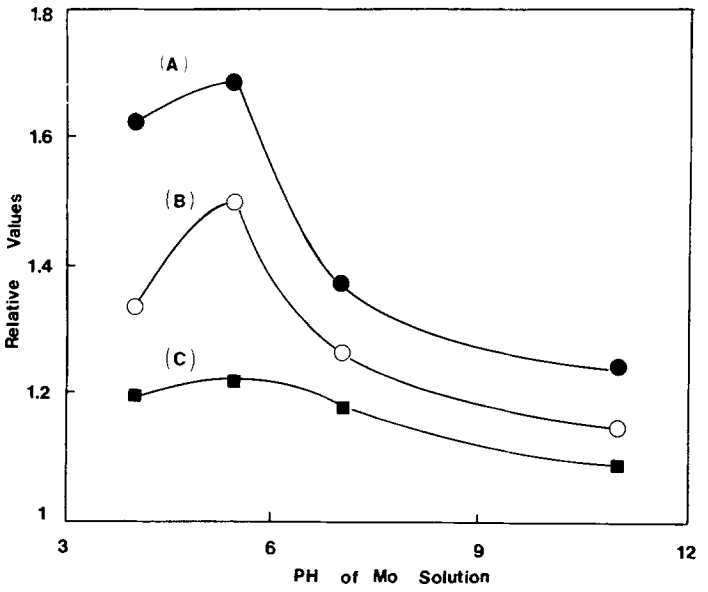

FIG. 7. Comparison of thiophene HDS activity with surface spectroscopic measurements. (A): ● Relative values of thiophene HDS activity expressed as half-order rate constant at steady state; (B): ○ Variation of ISS Mo/Al intensity ratio for the calcined catalyst; (C): ■ Variation of the ESCA Mo/Al intensity ratio for the calcined catalyst.

(I_{Mo}/I_{Al}) and the same variation trend as a function of pH. One may thus conclude that no significant modification of the repartition of the Mo phase take place as a result of changing the Mo impregnation pH.

Effect of Calcination

The observed increase in ESCA and ISS intensity ratios $I_{(Mo)}/I_{(Al)}$ as a result of calcination may be taken as an indication of better dispersion of the calcined Mo species. Redispersion of Mo species seems, thus, to accompany the breakup of the heptamolybdate during heat treatment. One can not, unequivocally, exclude the possibility that such increases in ESCA and ISS intensity ratios may, in principle, be ascribed to repartition effects (e.g., enrichment in Mo of the outer part of the catalyst particle as a result of the calcination treatment). However, a recent study (*14*) has shown that the reverse phenomenon occurs upon calcination, e.g., Mo migration from the surface into the interior.

An estimate of the degree of dispersion of Mo in the calcined samples may be obtained from Eq. (1) by comparing the observed ESCA intensity ratio, $I_{(Mo)}/I_{(Al)}$ = 0.8–0.9, with the value predicted for monolayer dispersion, $I_{(Mo)}/I_{(Al)}$ = 0.8. The result is in accord with the (postulated) nearly atomic dispersion of molybdena–alumina catalysts. However, because of the finite escape depth of Mo 3*d* electrons (ca. 1.6 nm), the predicted ESCA intensity ratio $I_{(Mo)}/I_{(Al)}$ for a monolayer will be essentially the same as the ratio for a highly dispersed MoO_3 phase (which has a thickness less than the escape depth). Thus, the ESCA results, while confirming the highly dispersed state of the Mo phase, cannot distinguish between a true monolayer and very small, highly dispersed crystallites of MoO_3.

Effect of Reduction

In a detailed study of the reduction of molybdena–alumina catalysts (*13*), it was shown that the reduction of octahedral Mo^{6+}, Mo(oct), leads to Mo^{4+}, whereas tetrahedral Mo^{6+}, Mo(tet), exclusively forms Mo^{5+}. The ratio of Mo(oct)/Mo(tet) was determined to be a function of Mo loading and calcination temperature. Our results suggest that when the catalysts are obtained by pore volume impregnation, the pH of Mo impregnating solution has little effect on the distribution of Mo between octahedral and tetrahedral sites.

Reduced molybdena–alumina catalysts all exhibit a slight decrease in the ESCA intensity ratio $I_{(Mo)}/I_{(Al)}$, compared to the corresponding calcined specimens. Assuming nearly atomic dispersion for the calcined samples, one may be tempted to conclude that reduction of Mo induces a slight disruption of the monolayer, thus exposing a higher fraction of Al to the surface. Indeed, based on infrared measurements, Fransen *et al.* (*16*), have shown that reduced molybdena–alumina catalysts exhibit new OH bands associated with the alumina. More recently, Millman *et al.* (*17*) similarly reported enhancement of the intensity of the OH band ascribed to alumina, as a result of reduction. Millman *et al.* proposed a reduction mechanism to account for "peeling" of the Mo monolayer from the surface. They presumed that hydrogen attacks the oxygens bonded to the alumina support instead of those in the capping layer (Scheme 1).

The Mo^{4+} species formed was assumed to remain bound to the support because of the observed difficulty in reducing Mo, in the case of molybdena–alumina, to oxidation states lower than Mo^{4+}. However, the magnitude of the observed decrease in ESCA intensity ratio $I_{(Mo)}/I_{(Al)}$ of about 20% cannot be accounted for solely on the basis of the proposed shrinkage of the Mo monolayer. Indeed, because of the relatively large escape depth of photoelectrons in the Al 2*p* level (about 1.8 nm) (*11*), the intensity of the Al 2*p* peak derives from the top seven layers. Moreover, the Mo loading is considerably below the nominal amount which corresponds to full monolayer cover-

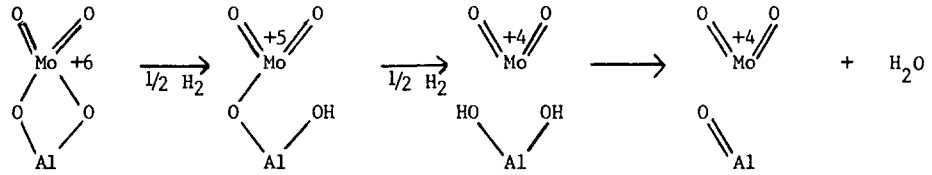

SCHEME 1

age (about 13% Mo). Therefore, the possibility of the formation of MoO_2 crystallites has to be considered.

Surface Structure and Catalytic Activity

Hydrodesulfurization activity of molybdena–alumina catalysts is a function of many parameters among which are (a) the nature of the Mo phase (e.g., MoO_3, Mo monolayer, polymolybdate), (b) its dispersion over the alumina carrier, (c) the symmetry of Mo species (e.g., tetrahedral or octahedral), and (d) the extent of sulfidation. It is, thus, unlikely to expect a simple correlation between activity and surface structure. However, in the case of the molybdena–alumina catalysts considered here, the variation of HDS activity seems to reflect the modification of dispersion brought about by the change in the pH of Mo impregnation (Fig. 7). Higher HDS activities were obtained for better dispersed, low pH preparations. The closer correlation obtained between the variation of HDS activity and that of ISS intensity ratio I_{Mo}/I_{Al} (Fig. 7) may be explained in terms of higher surface sensitivity of ISS compared to ESCA (sampling depths are, respectively, 0.2 and 1.5 nm). These results are consistent with those reported by Badilla-Ohlbaum and Chadwick (*18*). Indeed, by comparing the surface structure and activity of two molybdena–alumina catalysts obtained, respectively, at pH = 2 and 8, these authors also concluded that acidic impregnation enhances Mo dispersion and improves HDS activity.

Effect of Impregnation pH

Examination of ESCA and ISS data for the dried, calcined, and reduced MoAl samples clearly indicates that while decreasing the impregnation of pH from 11 to 4 has no dramatic effect on the architecture of the final catalysts, an improvement of Mo dispersion is nevertheless achieved. These results are in agreement with the conclusions of our recent study related to the influence of promoters (Ni, Ti) and preparation conditions on the properties of HDS catalysts (*19*). The findings may be interpreted in light of the mechanism of adsorption of Mo ions and the preparation method adopted in our study.

Assuming that no dissolution of the support takes place, alumina, because of its amphoteric character, adsorbs anions or cations, respectively, at pH values below or above its isoelectric point, pH = 8 (*20*). An illustrative example taken from Ref. (*20*) is shown in Fig. 8. It follows that in the case of molybdena–alumina catalysts where Mo is deposited on alumina via impregnation by a solution of ammonium heptamolybdate, the adsorption of $Mo_7O_{24}^{6-}$ or MoO_4^{2-} anions is favored at low pH. Indeed, in a recent study by Wang and Hall (*5*), it was shown that when molybdena–alumina catalysts were prepared by adsorption of molybdate from dilute solutions of $(NH_4)_6Mo_7O_{24}$, negligible amounts of Mo were retained by the alumina at high pH's while significant loadings were achieved in acidic media. In the case of pore volume impregnation used here, the above-mentioned finding would translate into a higher dispersion for low pH preparations, since they would presumably contain a higher fraction of adsorbed Mo (vs "deposited" Mo). Adsorbed Mo is expected to better resist migration and aggregation during drying and calcination. Our results seem to corroborate that interpretation. The fact that only a limited enhancement of disper-

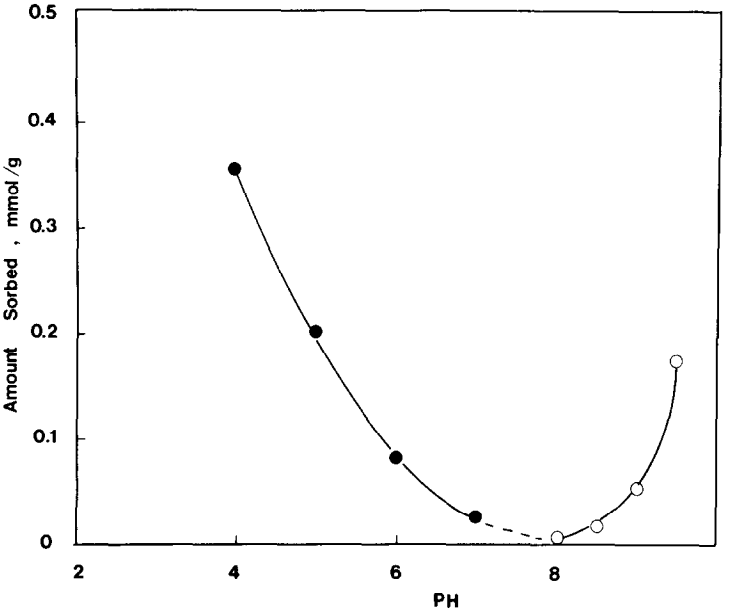

FIG. 8. Ammonium (○) and monochloroacetate (●) adsorption on γ-Al_2O_3 as a function of pH (Ref. (*20*)).

sion was observed at low pH may be ascribed (as pointed out by Wang and Hall) to the nature of the incipient wetness technique that was used for Mo impregnation. Because of the small volume of water involved in pore volume impregnation and the buffering capacity of alumina, addition of an aqueous solution of a Mo salt to the carrier would modify the initial pH of the Mo solution toward the carrier's isoelectric point (pH = 8 for alumina). Thus, while a substantial difference exists between the initial solution pH values, the equilibrated values will be much closer to one another. It is remarkable that the pH effect observed in the dried molybdena–alumina samples is maintained in the calcined, reduced, and reacted catalysts despite the redispersion of Mo species and the (expected) disruption of Mo ≪monolayer≫ resulting, respectively, from calcination and activation treatments.

A final remark should be made concerning the observed variations of ESCA and ISS intensity ratios $I_{(Mo)}/I_{(Al)}$ as a function of the impregnation pH. Based on the mechanism of adsorption of Mo species outlined above, one would expect that a decrease in the pH of impregnation from 11 to 4 should lead to a progressive increase in the dispersion of the Mo phase, which would be manifested by a steady enhancement of the measured ESCA and ISS intensity ratios. Our results show that while this is the case between pH = 11 and pH = 5.4, the trend seems to be reversed at lower pH (pH = 4). A tentative explanation of this phenomenon may be sought in the special features of acidic impregnation. Indeed, only in the case of the pH = 4 preparation did the making of the catalyst involve addition of nitric acid. The presence of nitrate ions may affect the repartition of the Mo phase over the alumina carrier and, thus, the ESCA and ISS intensity ratio $I_{(Mo)}/I_{(Al)}$. Furthermore, we observed that the adjustment of the pH of the Mo impregnating solution with nitric acid induced slight precipitation of the polymolybdate salt. That, in turn, will influence the ESCA and ISS relative intensity measurements.

ACKNOWLEDGMENT

This work was supported, in part, by the National Science Foundation under Grant CHE-8020001.

REFERENCES

1. Schuit, G. C. A., and Gates, B. C., *AIChE J.* **19,** 417 (1973).
2. Grange, P., *Catal. Rev. Sci. Eng.* **21,** 135 (1980).
3. Massoth, F. E., "Advances in Catalysis," Vol. 27, p. 265, Academic Press, New York, 1978.
4. Petrakis, L., Meyer, P. L., and Debies, T. P., *J. Phys. Chem.* **84,** 1029 (1980).
5. Wang, L., and Hall, W. K., *J. Catal.* **66,** 251 (1981).
6. Angevine, P. J., Vartuli, J. L., and Delgass, W. N., Proc. VIth Int. Cong. Cat. (G. C. Bond, P. Wells, and F. C. Tompkins, Eds.), Vol. 2, p. 611, The Chemical Society, London, 1976.
7. Defosse, C., Canesson, P., Rouxhet, P. G., and Delmon, B., *J. Catal.* **51,** 269 (1978).
8. Fung, S. C., *J. Catal.* **58,** 454 (1979).
9. Kerkhof, F. P. J. M., and Moulijn, J. A., *J. Phys. Chem.* **83,** 1612 (1979).
10. Scofield, J. H., *J. Electron Spectrosc. Relat. Phenom.* **8,** 129 (1976).
11. Penn, D. R., *J. Electron Spectrosc. Relat. Phenom.* **9,** 29 (1976).
12. Delannay, F., Houalla, M., Pirotte, D., and Delmon, B., *Surf. Interface Anal.* **1,** 172 (1979).
13. Zingg, D. S., Makovsky, L. E., Tisher, R. E., Brown, F. R., and Hercules, D. M., *J. Phys. Chem.* **84,** 2898 (1980).
14. Edmonds, T., and Mitchell, P. C. H., *J. Catal.* **64,** 491 (1980).
15. Defosse, C., *J. Electron Spectrosc. Relat. Phenom.* **23,** 157 (1981).
16. Fransen, F., Van der Meer, O., and Mars, P., *J. Catal.* **42,** 79 (1976).
17. Millman, W. S., Crespin, M., Cirillo, A., Abdo, S., and Hall, W. K., *J. Catal.* **60,** 404 (1979).
18. Badilla-Ohlbaum, R., and Chadwick, D., *Stud. Surf. Sci. Catal.* **7,** 1126–1140 (1981).
19. Houalla, M., Kibby, C., Petrakis, L., and Hercules, D. M., to be published.
20. Brunelle, J. P., *in* "Preparation of Catalysts II" (B. Delmon, P. Grange, P. Jacobs, and G. Poncelet, Eds.), p. 211, Elsevier, Amsterdam, 1979.